

Supporting Information

Table S1 Selected bond distances /Å and bond angles /° for **1-4**.

CP 1			
Zn(1)-O(9)	1.9011(17)	Zn(1)-O(6)	1.9733(15)
Zn(1)-O(3C)	1.9795(15)	Zn(1)-N(3D)	2.0393(18)
Zn(2)-O(9)	1.9345(16)	Zn(2)-O(1B)	2.0033(15)
Zn(2)-N(4)	2.097(2)	Zn(2)-N(5)	2.174(2)
Zn(2)-O(5)	2.1858(16)		
O(9)-Zn(1)-O(3C)	122.08(7)	O(9)-Zn(1)-O(6)	106.72(7)
O(9)-Zn(1)-N(3D)	103.61(8)	O(6)-Zn(1)-O(3C)	113.48(7)
O(3C)-Zn(1)-N(3D)	98.63(7)	O(6)-Zn(1)-N(3D)	111.40(7)
O(9)-Zn(2)-N(4)	124.33(8)	O(9)-Zn(2)-O(1)	111.09(7)
O(9)-Zn(2)-N(5)	93.45(7)	O(1B)-Zn(2)-N(4)	124.32(7)
N(4)-Zn(2)-N(5)	77.81(8)	O(1B)-Zn(2)-N(5)	95.05(7)
O(1B)-Zn(2)-O(5)	95.84(7)	O(9)-Zn(2)-O(5)	87.45(7)
N(5)-Zn(2)-O(5)	167.94(7)	N(4)-Zn(2)-O(5)	91.75(7)
CP 2			
Zn(1)-O(14)	1.942(3)	Zn(1)-O(7F)	1.972(3)
Zn(1)-O(10E)	1.975(3)	Zn(1)-N(6)	2.016(3)
Zn(2)-N(3)	2.032(3)	Zn(2)-O(3B)	1.982(2)
Zn(2)-O(5C)	1.986(3)	Zn(2)-O(15)	1.923(3)
Zn(3)-O(1)	1.956(3)	Zn(3)-O(9E)	2.431(3)
Zn(3)-O(13)	2.086(4)	Zn(3)-O(14)	1.964(3)
Zn(3)-N(8D)	2.041(3)	Zn(4)-N(7)	2.028(3)
Zn(4)-O(4B)	2.465	Zn(4B)-O(15)	1.932(3)
Zn(4)-O(16)	2.098(4)	Zn(4)-O(11)	1.932(3)
Zn(4)-N(7)	2.028(3)		
O(14)-Zn(1)-O(7F)	112.28(12)	O(14)-Zn(1)-O(10E)	112.50(12)
O(7F)-Zn(1)-O(10E)	106.67(11)	O(14)-Zn(1)-N(6)	105.18(13)
O(7F)-Zn(1)-N(6)	103.95(12)	O(10E)-Zn(1)-N(6)	116.07(13)
O(15)-Zn(2)-O(3B)	113.41(12)	O(15)-Zn(2)-O(5C)	116.45(12)
O(3B)-Zn(2)-O(5C)	107.91(11)	O(15)-Zn(2)-N(3)	102.61(14)
O(3B)-Zn(2)-N(3)	112.96(13)	O(5C)-Zn(2)-N(3)	103.03(13)
O(1)-Zn(3)-O(14)	105.08(12)	O(1)-Zn(3)-N(8D)	143.03(13)
O(14)-Zn(3)-N(8D)	109.83(12)	O(1)-Zn(3)-N(13)	98.74(14)
O(14)-Zn(3)-O(13)	95.80(13)	N(8D)-Zn(3)-O(13)	89.60(15)
O(1)-Zn(3)-O(9E)	89.37(12)	O(14)-Zn(3)-O(9E)	84.24(11)

N(8D)-Zn(3)-O(9E)	82.47(12)	O(13)-Zn(3)-O(9E)	171.56(12)
O(15)-Zn(4)-O(11)	110.90(13)	O(15)-Zn(4)-N(7)	110.57(13)
O(11)-Zn(4)-N(7)	135.03(13)	O(15)-Zn(4)-O(16)	97.89(13)
O(11)-Zn(4)-O(16)	94.46(15)	N(7)-Zn(4)-O(16)	96.40(16)
O(15)-Zn(4)-O(4B)	84.06(11)	O(11)-Zn(4)-O(4B)	86.10(12)
N(7)-Zn(4)-O(4B)	81.60(13)	O(16)-Zn(4)-O(4B)	177.61(12)
CP 3			
Cu(1)-O(7)	1.896(2)	Cu(1)-O(1)	1.9745(17)
Cu(1)-O(5C)	1.9808(17)	Cu(1)-N(3)	2.041(2)
Cu(2)-O(7)	1.9357(19)	Cu(2)-O(3B)	2.0029(17)
Cu(2)-N(4D)	2.099(2)	Cu(2)-N(5)	2.173(2)
Cu(2)-O(2)	2.1848(18)		
O(7)-Cu(1)-O(1)	106.69(8)	O(7)- Cu(1)-O(5C)	122.00(8)
O(1)- Cu(1)-O(5C)	113.47(8)	O(7)- Cu(1)-N(3D)	103.61(9)
O(1)- Cu(1)-N(3D)	111.36(8)	O(5C)- Cu(1)-N(3D)	98.81(8)
O(7)- Cu(2)-O(3B)	111.08(8)	O(7)- Cu(2)-N(4)	124.36(9)
O(3B)- Cu(2)-N(4)	124.31(8)	O(7)- Cu(2)-N(5)	93.54(9)
O(3B)- Cu(2)-N(5)	94.99(8)	N(4)- Cu(2)-N(5)	77.85(9)
O(7)- Cu(2)-O(2)	87.43(8)	O(3B)- Cu(2)-O(2)	95.97(7)
N(4)-Cu(2)-O(2)	91.59(8)	N(5)- Cu(2)-O(2)	167.84(8)
CP 4			
Cu(1)-O(3D)	2.176(4)	Cu(1)-O(2)	1.986(4)
Cu(1)-O(4)	1.905(3)	Cu(1)-N(5)	2.062(5)
Cu(1)-N(4)	2.016(6)		
O(2)- Cu(1)-O(3D)	101.07(18)	O(27)- Cu(1)-N(5)	155.48(19)
O(2)- Cu(1)-N(4)	91.2(2)	O(4)- Cu(1)-O(3D)	94.79(19)
O(4)- Cu(1)-O(2)	92.57(15)	O(4)- Cu(1)-N(5)	94.12(17)
O(4)- Cu(1)-N(4)	174.89(19)	N(5)- Cu(1)-O(3D)	101.84(19)
O(3D)- Cu(1)-N(4)	87.9(2)	N(4)- Cu(1)-N(5)	81.0(2)

Symmetric codes: A: -x, -y, -z; B: 1+x, y, z; C: x, -1+y, z; D: 1-x, 1-y, 1-z; for **1**; A : -x, -y, -z; B: 2-x, 2-y, -z; C: 1-x, 2-y, -z; D: x, 1+y, 1+z; E: 2-x, 2-y, 1-z; F: 3-x, 2-y, 1-z for **2**; A: -x, -y, -z ; B: -1+x, y, z; C: x, 1+y, z; D: 1-x, 1-y, 1-z for **3**; A: -x, -y, -z ; B:-x, y, -z+1/2 ; C: x+1/2, y+1/2, z; D: -x+1/2, y+1/2, -z+1/2 for **4**.

Table S2 Hydrogen bond distances (\AA) and bond angles ($^\circ$) for **2**

$D\text{-}H\cdots A$	$d(D\cdots A)$	$\angle(DHA)$
O18-H18B...O23	2.751(2)	122(2)
O16-H16A...O18	2.743(2)	152(2)
O16-H16B...O23	2.792(2)	170(2)
O23-H23A...O22	2.906(2)	158(3)
O17-H17B...O19	2.666(2)	178(3)
O17-H17A...O2	2.733(2)	172(2)
O22-H22B...O17	2.978(2)	177(2)
O13-H13B...O17	2.722(2)	162(3)
O22-H22A...O6	2.754(2)	168(3)
O23-H23A...O24	2.804(2)	163(3)
O24-H24A...O23	2.963(2)	120(2)
O20-H20A...O19	2.703(2)	135(2)
O20-H20B...O3	2.935(2)	119(2)

Fig. S1 View of the 3D supramolecular architecture based on $\pi \cdots \pi$ stacking interactions along a -axis.

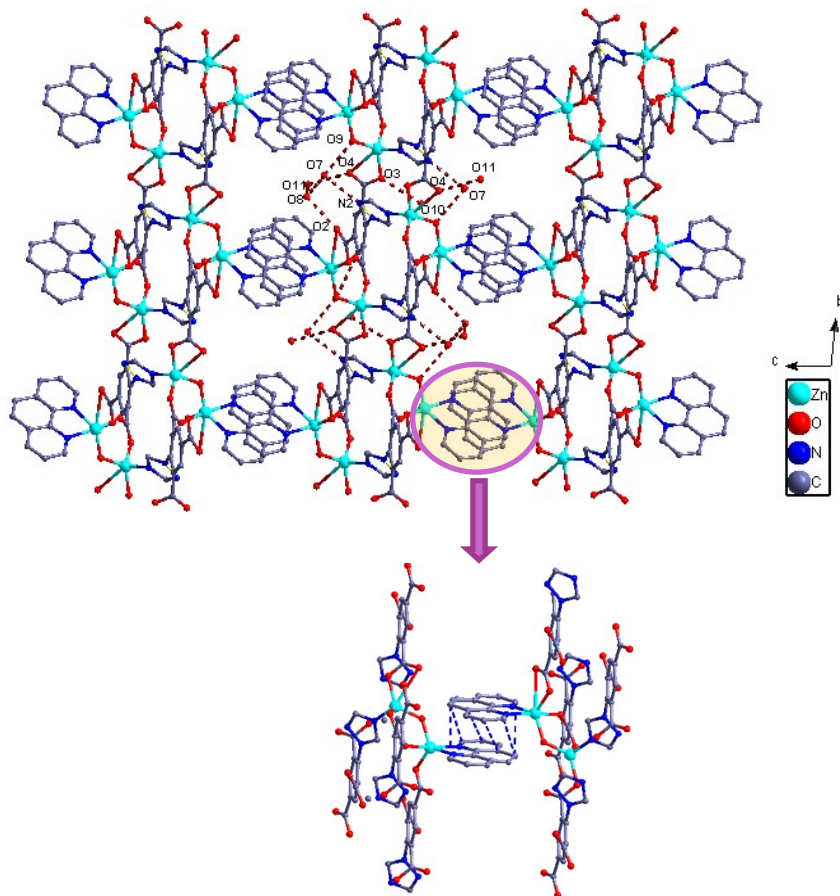
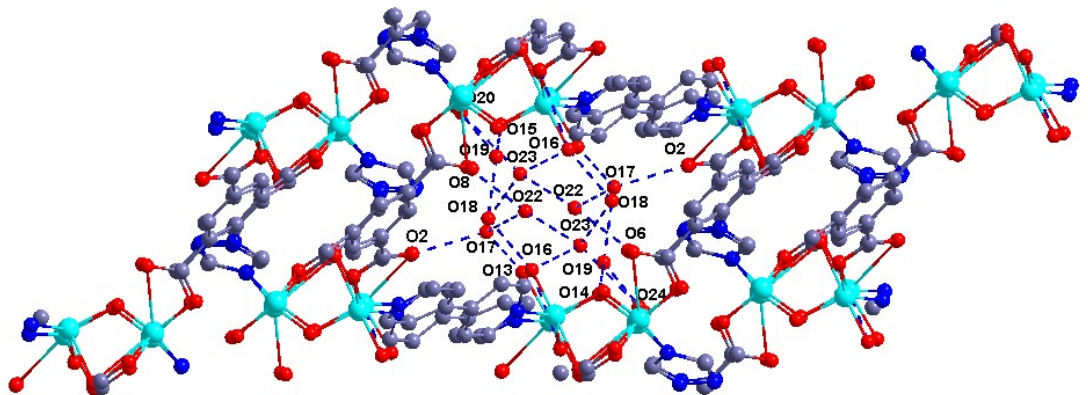
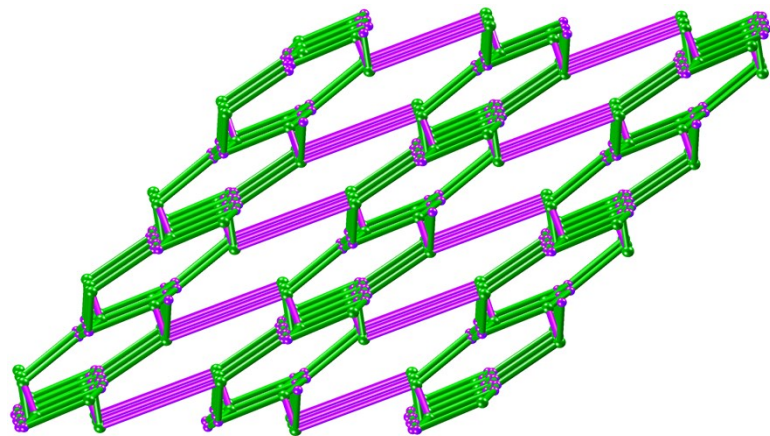


Fig. S2 (a) View of water clusters based on hydrogen bonding interactions in 3D network along *c*-axis. (b) View of topological structure of 3D network.



(a)



(b)

Fig. S3. TGA curves of CPs 1-4.

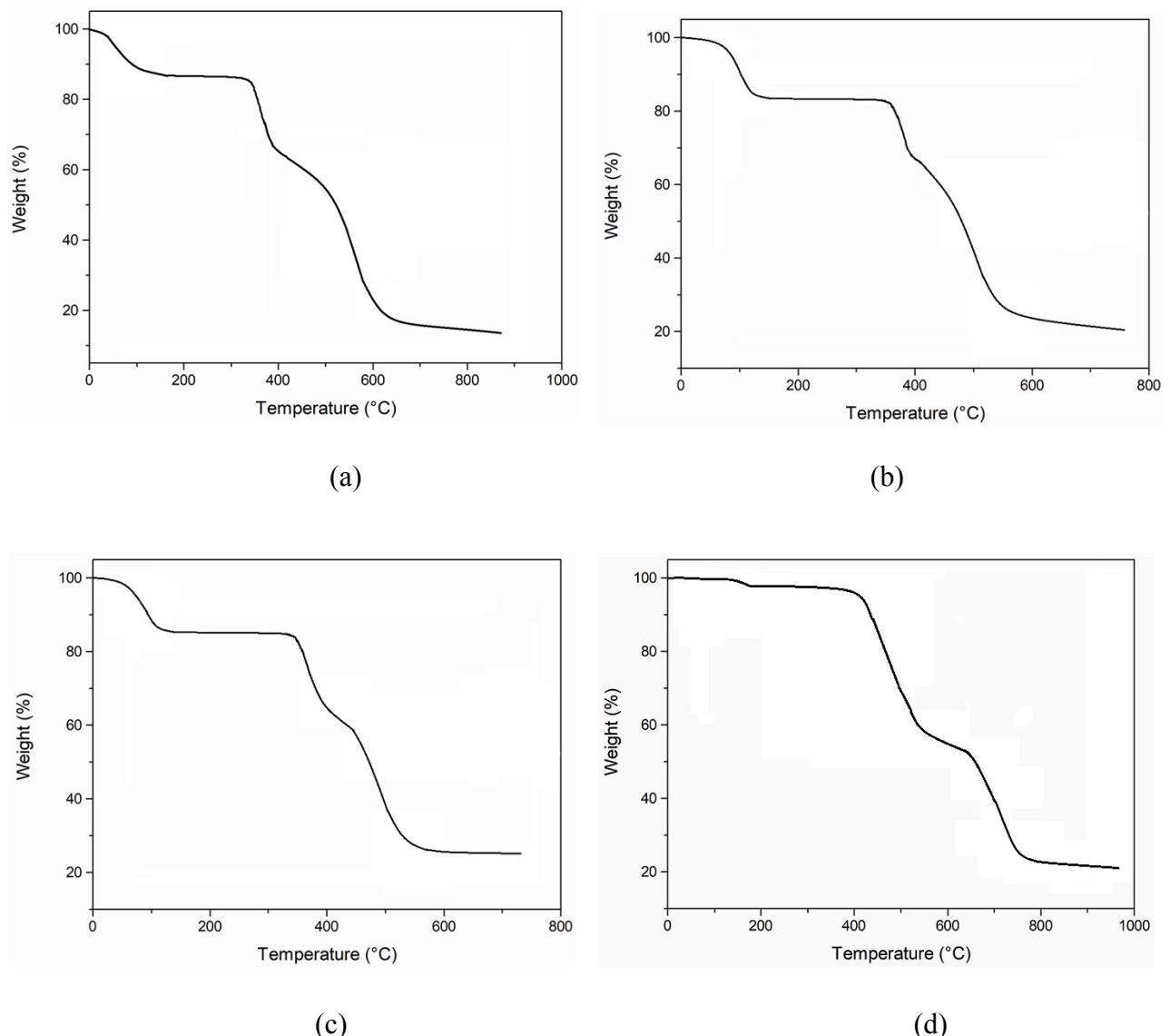


Fig. S4. PXRD patterns of CPs **1-4**.

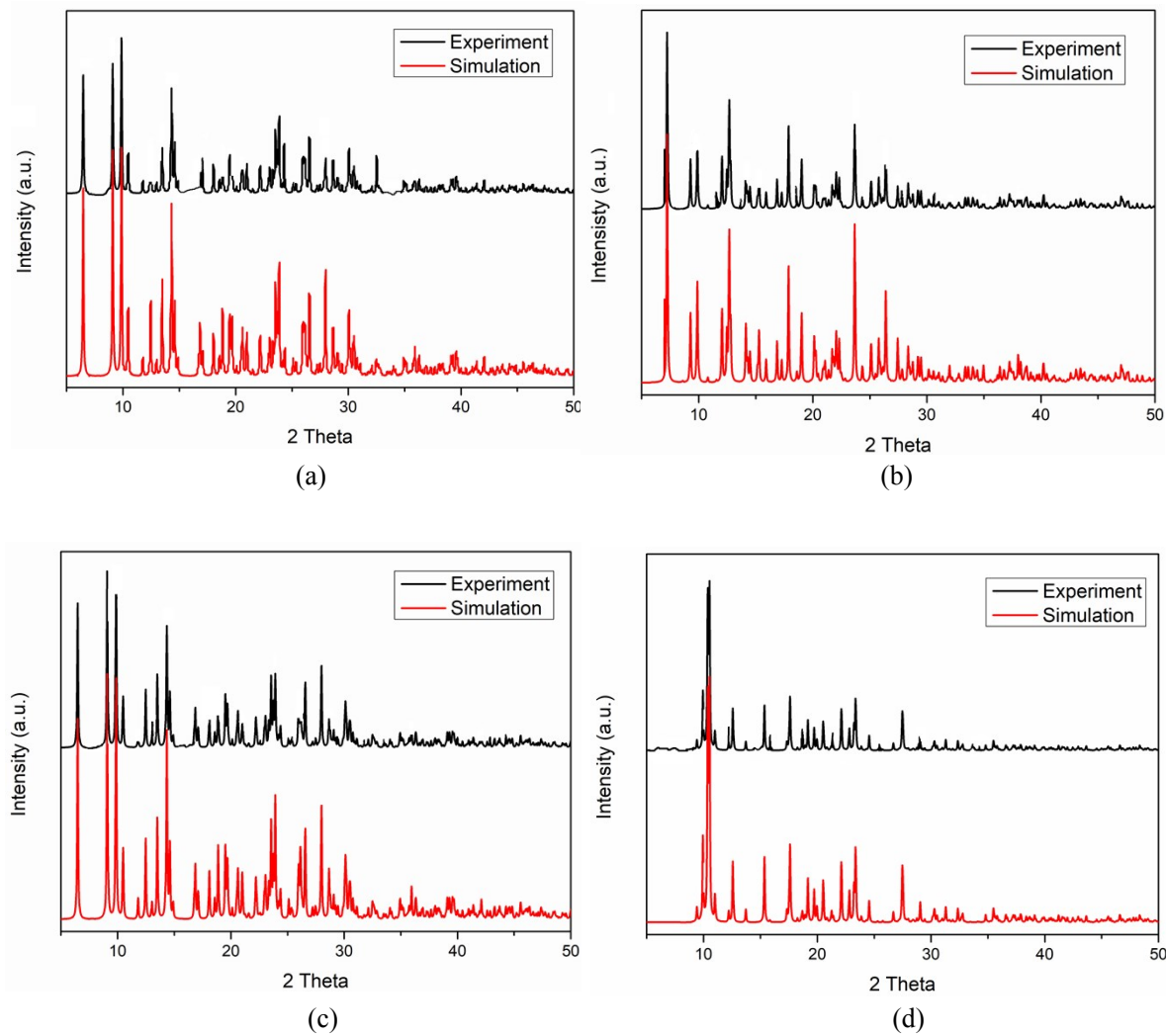


Fig. S5 Emission intensities of **1** dispersed in the aqueous solution of Cu^{2+} in the presence of different ions.

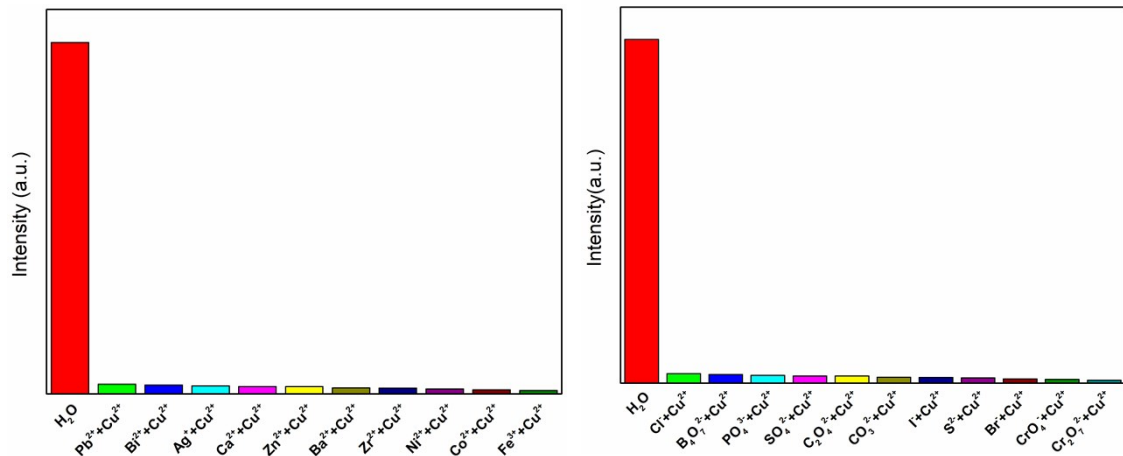


Fig. S6 (a) linear plot of $I_0/I-1$ and low Cu^{2+} concentration. (b) linear plot of $I_0/I-1$ and low $\text{Cr}_2\text{O}_7^{2-}$ concentration.

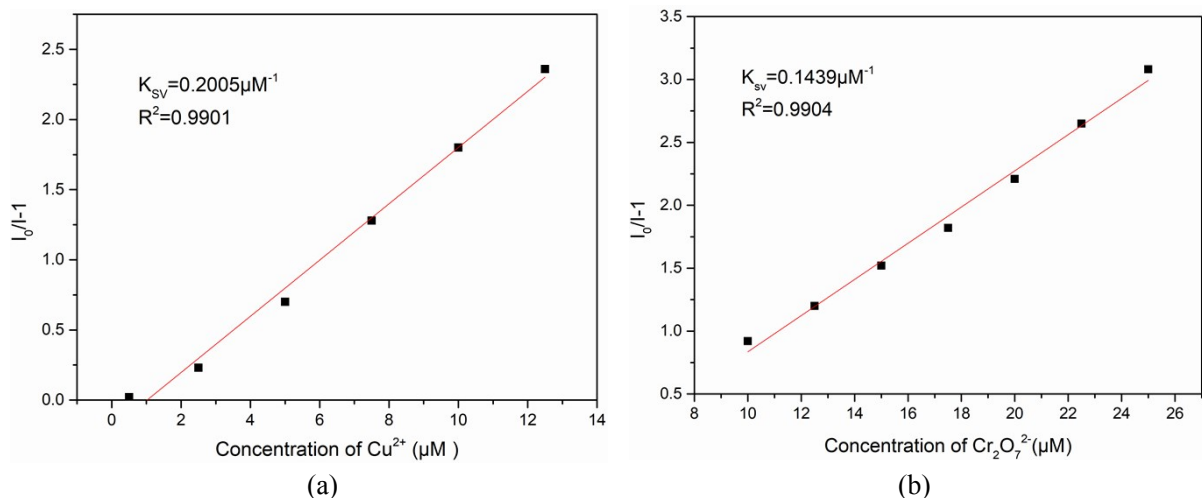


Fig. S7 Emission intensities of **1** dispersed in the aqueous solution of $\text{Cr}_2\text{O}_7^{2-}$ in the presence of different ions.

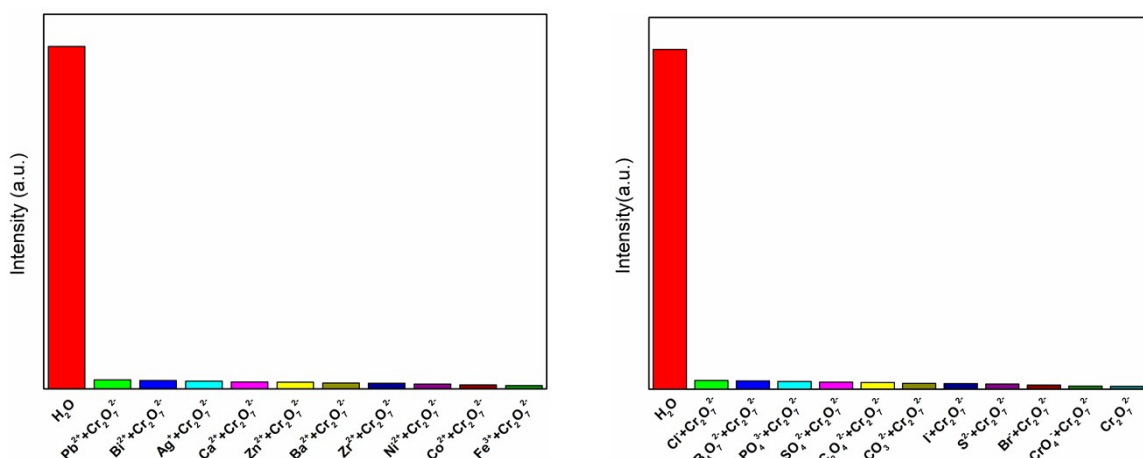


Fig. S8 The UV-vis spectra (a: metal ions; b: anions; insert section: the excitation spectra of 1).

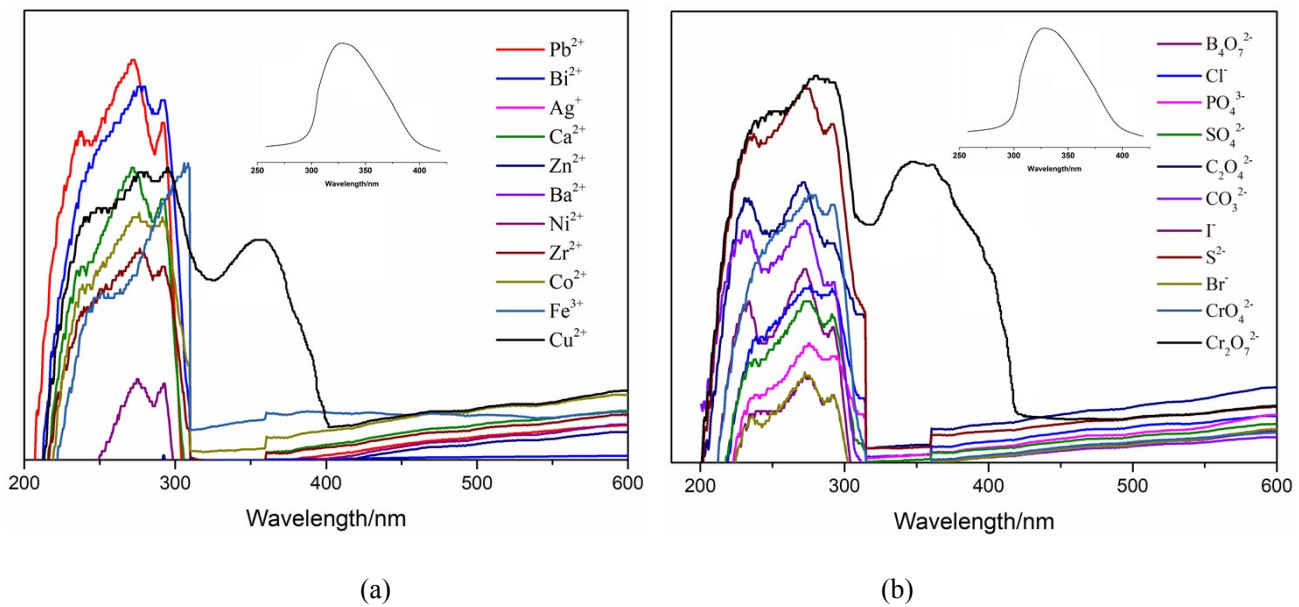


Fig. S9 The luminescence intensity of 1 after sensing experiments (a: Cu^{2+} ; b: $\text{Cr}_2\text{O}_7^{2-}$) four runs of recycling.

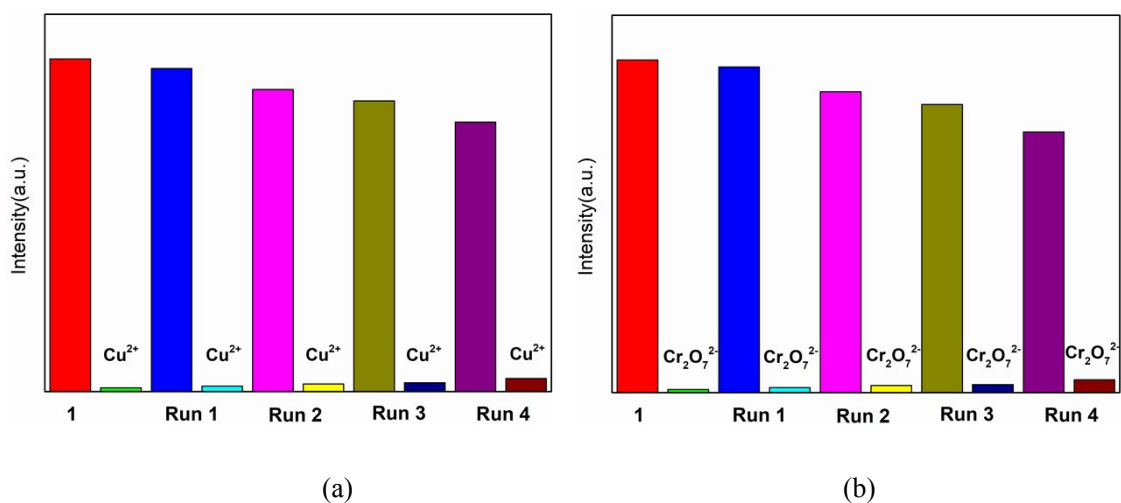


Fig. S10 The PXRD patterns (a: 1 after sensing Cu²⁺ for four cycles in H₂O; b: 1 after sensing Cr₂O₇²⁻)

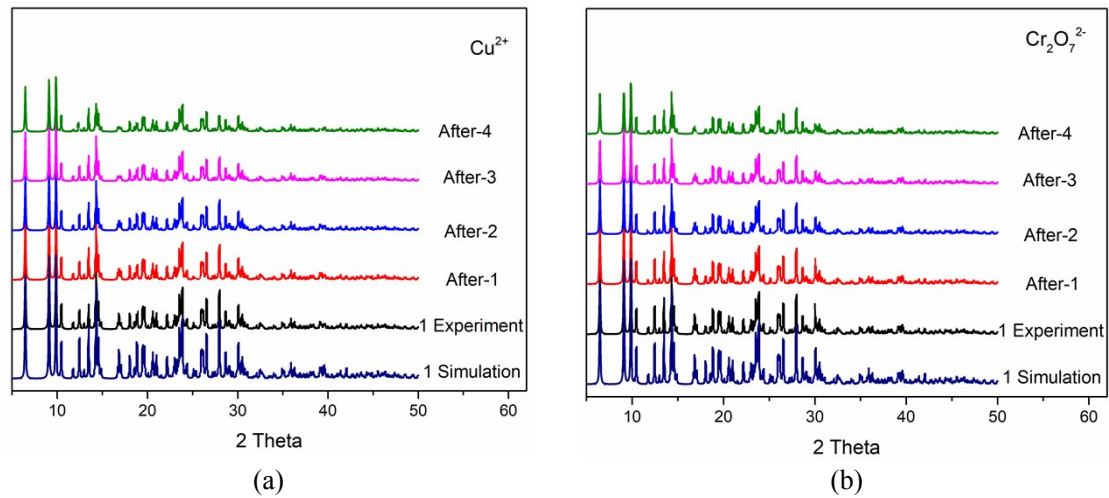


Fig. S11. UV-vis diffuse-reflectance spectra of CPs **3-4** with BaSO₄ as background.

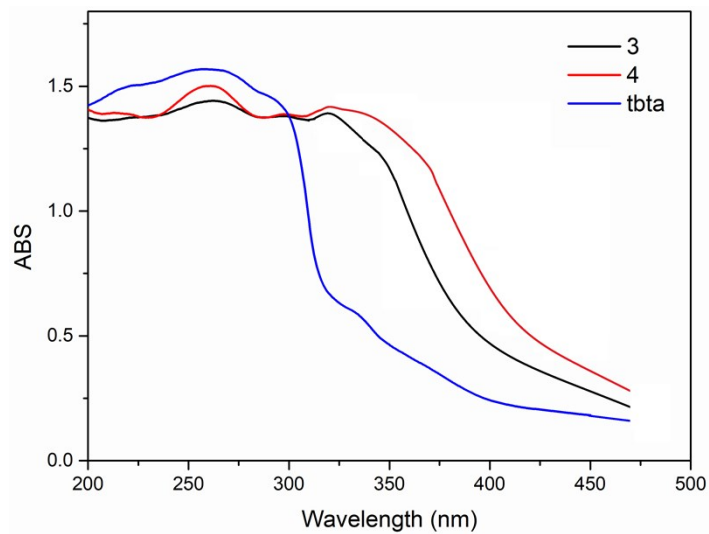


Fig. S12. Kubelka Munk-transformed diffuse reflectance spectra of 3(a) and 4(b).

